JACS Au
AN OPEN ACCESS JOURNAL OF THE AMERICAN CHEMICAL SOCIETY

pubs.acs.org/jacsau

Perspective

Fluid-Mediated Fabrication of Complex Assemblies

Pierre-Thomas Brun*

Cite This: *JACS Au* 2022, 2, 2417−2425

Read Online

ACCESS | Metrics & More | Article Recommendations

ABSTRACT: This Perspective accounts for recent progress in the directed control of interfacial fluid flows harnessed to assemble architected soft materials. We are focusing on the paradigmatic problem of free-surface flows in curable elastomers. These elastomers are initially liquid and cure into elastic solids whose shape is imparted by concomitant and competing phenomena: flow-induced deformations and curing. Particular attention is given to the role of capillary forces in these systems. Originating from the cohesive nature of liquids and thus favoring smooth interfaces, capillary forces can also promote the destabilization of interfaces, e.g., into droplets. In turn, such mechanical instabilities tend to grow into regular patterns, e.g., forming hexagonal lattices. We discuss how the universality, robustness, and ultimate regularity of these out-of-equilibrium processes could serve as a basis for new fabrication paradigms, where instabilities are directed to generate target architected solids obtained without each element laid in place by direct mechanized intervention.

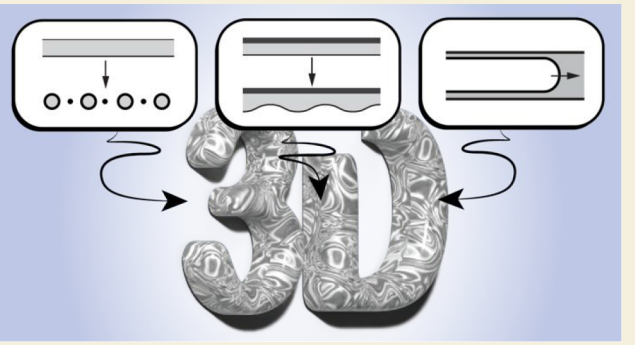

KEYWORDS: *interfacial flows, 3D printing, capillarity, polymer, curing, pattern, instability*

HARNESSING INTERFACIAL FLOWS

Since the Bronze Age, humans have used the inherent compliance of liquids to shape materials and fabricate artifacts. Metal casting, glass blowing, and even painting are all processes where a final construct is obtained following the solidification of an initially liquid phase shaped by a combination of tools and craftsman skills. Throughout history, this concept has matured into a plethora of industrial processes that often rely on mechanized intervention *and* interfacial effects unique to liquid phases. For instance, capillary forces are routinely used to straighten interfaces, e.g., in dip coating[1] and the glass float process,[2] and to disperse liquids, e.g., in inkjet printing[3] and atomization.[4] Due to favorable downscaling with length, the idea of harnessing interfacial effects for materials design is also gaining momentum in the laboratory, e.g., through the use of microfluidic emulsions,[5−8] capillary-mediated self-folding,[9−13] and interfacial instabilities in molten phases[14] (see Figure 1). While the former examples have been vigorously researched, the literature on interfacial fluid mechanics in solidifying liquids remains sparse, leaving the outstanding scientific question of the relation between flow and shape mostly unanswered.[15] Specifically, predictive theoretical models accounting for the concomitant and competing phenomena at play in the formation of morphological structures are often lacking due to the multiphysics complexity of these phenomena.

Additionally, interfacial instabilities are often studied close to threshold such that pattern formation in these systems remains poorly understood. Here we survey recent experimental and theoretical efforts to fill this knowledge gap. In particular, we discuss how and when this class of fluid-mediated fabrication methodologies can advantageously complement existing approaches for assembling structures and structural heterogeneities in macroscopic systems, e.g., 3D printing;[16,17] and microscopic techniques, e.g., photolithography,[18] nanopatterning,[19] and other kinds of self-assembly approaches.[20] To this day, producing complex multimaterial assemblies with multiscale structures ordered from the nanoscale to the microscale and macroscale remains technologically challenging.[21] New paradigms are thus needed to enable the flexible and scalable fabrication of such bioinspired materials, whose fibrous, layered, gradient, cellular, and interlocking architectures could be leveraged[22,23] to perform advanced functions including self-cleaning, drag reduction, light coloration, camouflage, sound manipulation, insulation, sensing, high mechanical strength, and other advanced mechanical properties and programmable shape change.

Received: August 1, 2022
Revised: October 3, 2022
Accepted: October 3, 2022
Published: October 24, 2022

https://doi.org/10.1021/jacsau.2c00427
JACS Au 2022, 2, 2417−2425

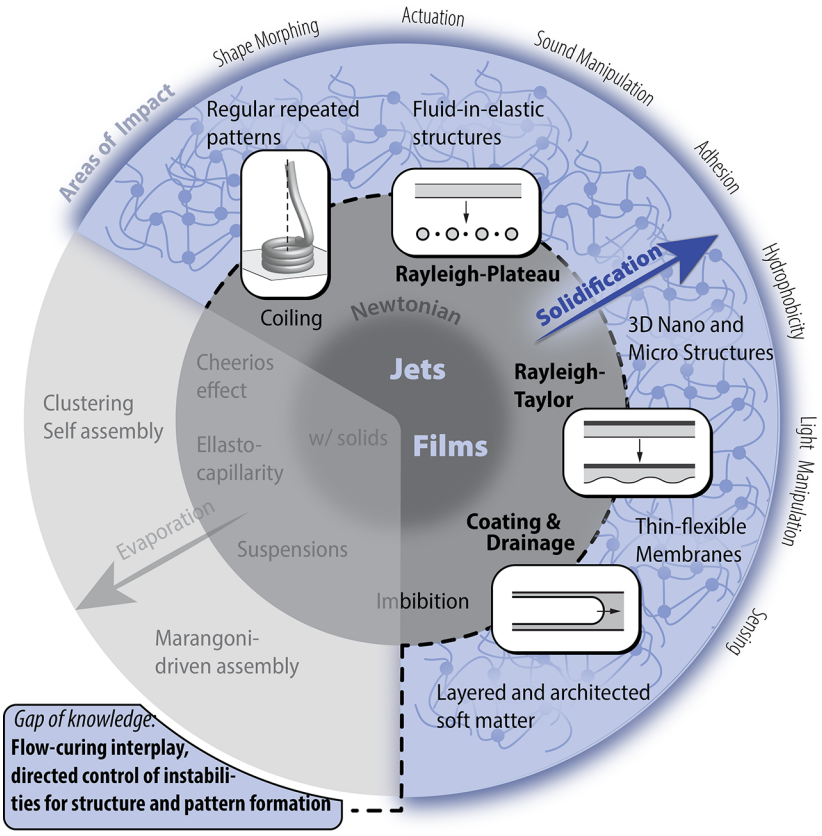

Figure 1. From liquid to functional solids. We discuss the possibility of harnessing interfacial flows in solidifying melts to assemble structured solids. Particular attention is given to devising strategies for the directed control of stable and unstable flows and the shapes and patterns they produce.

PATTERN FORMING SYSTEMS

In nature, organized arrays of elements arise spontaneously from the interactions between their parts, e.g., reaction-diffusion problems,[24] clustering particles and granular media,[25,26] wrinkling surfaces,[27] propagating cracks,[28] and, of particular interest to this article, flowing liquids and interfaces.[14] Such structures are universally self-organized, a property that could be advantageously leveraged in engineering settings. For instance, the coils that form when honey impinges a toast at breakfast emerge from a buckling instability[29,30] (Figure 2). Therefore, these coils do not require an operator to move into carefully controlled circles. These patterns are universal and transcend the traditional divisions between scientific fields. For instance, coiling structures are seen in systems that might seem to have nothing in common, such as an elastic rope[31,32] and a viscous thread,[30,33−35] while their scale ranges from a micrometer[36] and less[37] to meters.[31] These similarities result from the mathematical analogies in the rules that govern such pattern formation.[30] In effect, it was shown that a single scalar parameter could effectively rationalize these coiling patterns, that is, the ratio between the terminal speed of the thread at the contact point and the speed of the substrate relative to the nozzle from where the thread is extruded. Such simple and robust guideline could be helpful to practitioners, e.g., to fabricate foams with carefully controlled porosity,[38,39] even in materials as complex as molten glass in the midst of solidification.[40] Here we discuss the control of the multiple facets of complex out-of-equilibrium pattern forming phenomena in stable and unstable configurations. We primarily focus on the paradigmatic case where those patterns are harnessed in silicone-based elastomers that are initially liquid and solidify into elastic materials. Examples include polydimethylsiloxane (PDMS, Sylgard 184, Dow Corning) and vinylpolysiloxane (VPS, Elite Double 8, 16, and 32, Zhermack). These commercial elastomers are cross-linked materials that contain inorganic fillers (silica particles) and other additives (silicone oil). The mechanical properties of these polymers are greatly enhanced by cross-linking. Cross-linking is typically achieved by a reaction between vinyl end groups in the base and Si−H groups in the cross-linker via platinum catalyzed hydrosilylation.[41] These cross-linked elastomers are widely used across fields. Examples range from soft lithography,[18] an essential process in many microfluidic and microelectromechanical systems, to capturing highly accurate impressions in

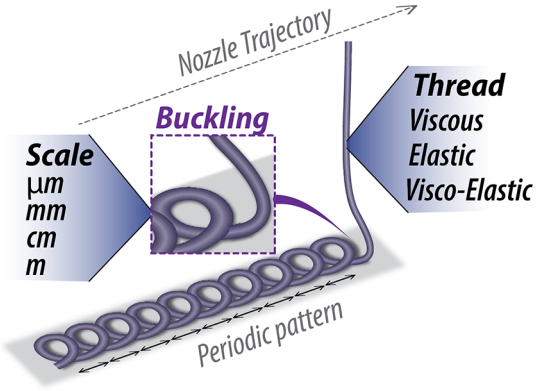

Figure 2. Coiling is universal. Coiling can is found across length scales and material properties, yielding regularly spaced patterns stemming from the buckling dynamics of a thread.

https://doi.org/10.1021/jacsau.2c00427
JACS Au 2022, 2, 2417−2425

dentistry. In all cases, elastomers are praised for their moldability. Here, we are interested in another facet of their nature, which pertains to the change of their viscosity over time. Specifically, these cross-linking mixtures tend to exhibit a snap-set behavior defined as the nearly constant maintenance of their viscosity followed by a rapid transition to elasticity. This rapid change is best captured by the following doomsday equation:[42]

$$\mu = \mu_0(1 - t/\tau_c)^{-n} \quad (1)$$

where τ_c is the curing time, μ_0 is the value of the initial viscosity, and n is a real number. In Figure 3, we show that eq 1 with $n = 2$

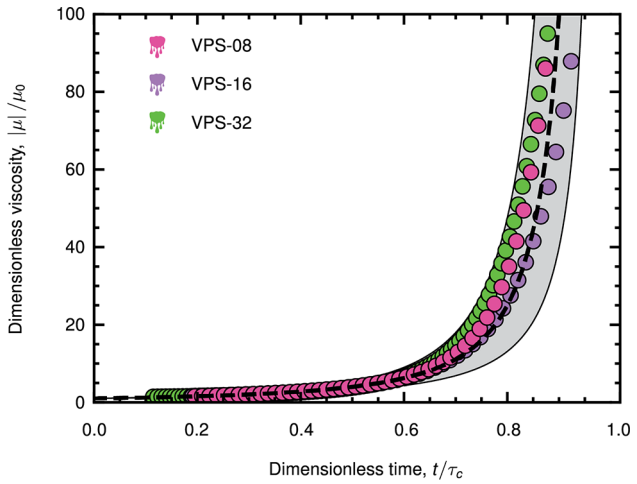

Figure 3. Viscosity of VPS elastomers. Rescaled viscosity of VPS-08, -16, and -32 solutions based on oscillatory shear rheology measurements. The dashed line corresponds to eq 1 with $n = 2$.

compares favorably with the viscosity of various VPS mixtures whose rheology was determined experimentally.[43] The initial viscosity of these polymers is typically of the order a few Pa·s, while their curing time may range from ∼600 s for VPS-08 and -16 to ∼1100 s for VPS-32.[43] Additionally, the viscosity of these solutions appears to be weakly affected by shear.[44] In the following, we show how the advantageous snap-set rheology of these elastomers can be leveraged to turn fluid flows into elastic structures with continuously tunable properties.

THIN FILMS

As inferred by its name, surface tension tends to straighten interfaces. As such, interfacial effects have long been leveraged to produce smooth interfaces when a thin layer of liquid is applied to a solid. For such coatings, the common practice is to help the process with some movement, e.g., by pulling the solid of a bath or rotating it. In both cases, the coating thickness is dictated by the hydrodynamics of the problem. For instance, the amount of fluid deposited on a substrate pulled out of a bath[1] is directly related to the speed of extraction U, the viscosity of the fluid μ, its density ρ, the acceleration of gravity g, and the surface tension of the liquid σ. In fact, the coating thickness is $h \propto l_c Ca^{2/3}$ with $l_c = \left(\frac{\sigma}{\rho g}\right)^{1/2}$ being the capillary length and $Ca = \frac{\mu U}{\sigma}$ being the capillary number (in the limit $Ca \ll 1$). Such coating thicknesses typically range from a few millimeters down to tenths of micrometers. In the laboratory, thinner coatings are attainable using a spin coater, where a layer with initial thickness h_0 will evolve as $h(t) = h_0/(1 + 4\rho\omega^2 h_0^2 t/3\mu)^{1/2}$ in the Newtonian limit, with ω the rotation speed.[45] It is of particular interest to applications because this flow will lose all *memory* of its initial condition, which is typically *not* uniform. As a result, for long enough times, the coating will converge to a universal uniform solution $h(t) \sim (3\mu/4\rho\omega^2 t)^{1/2}$ (ignoring other effects such as evaporation). Similar solutions can be found in passive settings, e.g., where gravity alone drives the flow so that the operator does not directly enforce the relative motion between solid and fluid. For instance, in the drainage of a viscous liquid coated on top of a sphere with radius R, the thickness varies as $h \simeq \sqrt{\frac{\mu_0 R}{\rho g t}}$. This solution[44] is agnostic of the initial thickness applied to the sphere and its ineffable lack of uniformity. Additionally, this universal law shows little dependence on the azimuthal angle, yielding virtually uniform coatings. Of particular interest for fabrication, these flows can be arrested in curable elastomers that are initially liquid and progressively cure to form elastic solids. Their typical rheology is well captured by[42]eq 1 using n=2. After curing is complete, a solid shell with uniform thickness is thus obtained. The shell thickness[44] is accurately captured by $h_f = \sqrt{\frac{3\mu_0 R}{4\rho g \tau_c}}$. In turn, this predictive knowledge can be leveraged to continuously tune the shell thickness by modifying the time between polymer preparation and the moment of pouring. The resulting shells are virtually free

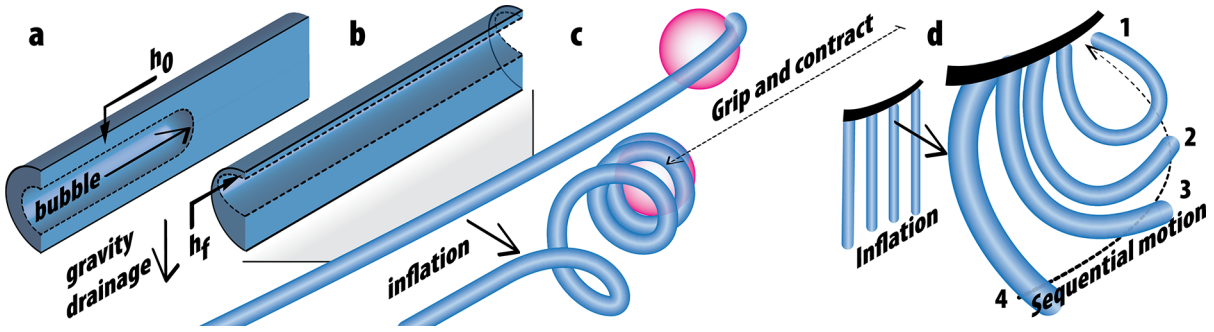

Figure 4. Bubble casting. (a) A cavity is carved by injecting a bubble into a cylinder initially filled with a liquid elastomer. (b) Gravity-induced drainage yields an anisotropic cross-section which eventually cures into a solid actuator. (c) Upon inflation, the actuator curls and can be used to grip a ball (pink), which is then carried as the actuator contracts. (d) Leveraging our model of the fabrication process enables us to program the actuator, e.g. displaying a sequential motion of 4 digits when inflated at once.

https://doi.org/10.1021/jacsau.2c00427
JACS Au 2022, 2, 2417−2425

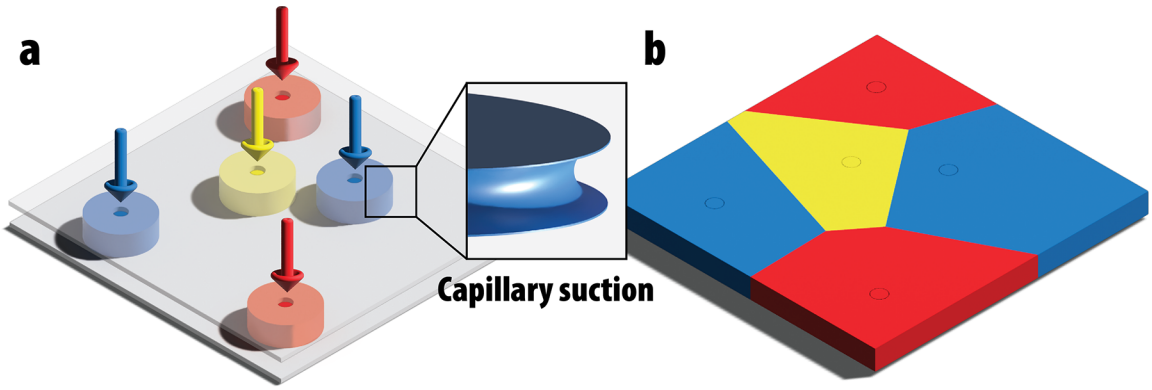

Figure 5. Pixelated sheets. (a) Liquid elastomers are poured on top of a Hele-Shaw cell composed of two rigid plates, with the top one presenting a series of holes. Inset: Capillary forces yield to the polymer imbibition. (b) The flows meet and form "pixels" whose shape matches the Voronoi mesh of the holes' positions. Vents (not shown) are located at the edges of the mesh.

of defects, i.e., making them more resistant to buckling[46,47] than would have been the case if fabricated using another fast prototyping approach, e.g., with 3D printing. These assets also make free-surface flows of curable polymers good candidates for the fabrication of soft robots, as detailed next.

BUBBLE CASTING

Soft robots are inspired by living organisms and developed from intrinsically compliant materials. Where conventional robots rely on hinges and bolts to achieve movement, soft robots use elastomeric actuators programmed to change shape following the application of stimuli, for example, pneumatic inflation, and perform continuous motions that mimic animal and vegetal movement. Note that the programming of these actuators is typically encoded in the shape of the actuator. As such, recent advances in rapid prototyping techniques have greatly facilitated the development of the field, e.g., enabling the fabrication of complex molds used to cast soft actuators. However, these fabrication processes have limitations in scalability, design flexibility, and robustness. An alternative approach has recently been reported, demonstrating that it is possible to harness interfacial flows in curable elastomers to produce monolithic pneumatic actuators. Leveraging the rules and tools of fluid mechanics, one can tailor their shape, making them suitable for applications ranging from artificial muscles to grippers. This approach, called "bubble-casting"[43] combines the physics of the aforementioned forced wetting and drainage flows. First, a tubular mold is filled by injecting uncured elastomer melt. While the melt is still liquid, air is injected to form an elongated bubble that creates the inner void of the actuator (Figure 4a). This annulus' thickness h_0 scales with the capillary number $Ca = \mu_0 U\sigma$, where U denotes the speed at which the bubble was pushed, μ_0 is the initial viscosity of the elastomer, and σ is its surface tension. In effect, we have $h_0 \sim RCa^{2/3}/(1 + Ca^{2/3})$, where R is the radius of the mold. In a typical experiment, $Ca \geq 1$, so that $h \sim 0.35R$. Note that the value of 35% is effectively a plateau so that monitoring the exact velocity of the bubble to predict h is not required so long as the bubble is fast enough to ensure $Ca \geq 1$". This robust result translates into a void fraction of about 50%. Gravity then sculpts the actuator by draining the polymer film and allowing the bubble to rise (Figure 4b). The drainage leaves a film with thickness:

$$h_f = 3\sqrt{\frac{\mu_0 R}{2\rho g \tau_c}\left(\frac{\tau_c}{\tau_c - \tau_w}\right)^3} \tag{2}$$

where τ_c is the polymer curing time and τ_w is the work time, i.e., the time elapsed between the mixing of the reagents and when the bubble is pushed into the mold.[43] The solution in eq 2 can be matched to that of the thick part of the actuator, which is obtained by integrating the Young−Laplace equation that follows the balance between gravity and capillarity. The final elastic cross-section obtained after curing is thus anisotropic. When inflated, the thin film deforms more than the rest of the structure, thereby inducing bending.[43] Considerable deformations are obtained such that a rod can grip around an object and lift it by contracting its effective length (see Figure 4c). Note that the cross section and its subsequent deformations can be tuned with mathematical precision. In particular, modifying the work time τ_w is a simple way to alter h_f (see eq 2). In turn, h_f dictates the response of these actuators to inflation. All other parameters remaining equal, the thinner h_f is, the higher the curvature is when inflation occurs. As such, merely assigning different values of τ_w in specific regions of the actuator will translate in an actuator with a distribution of curvatures upon inflation. This property can be leveraged to program an actuator, e.g., generating a sequential motion (see Figure 4d). In such a case, the *program* is embedded into the *shape* of the actuator which has been engineered leveraging the rules and tools of fluid mechanics. In particular, these monolithic constructs have smooth membranes with thickness on the order of 100 μm, which are virtually uniform over meter-long samples. Additionally, the active part of the fabrication, i.e. the bubble injection, only takes seconds, while curing is typically achieved in 10 min. Those time scales reflect the potential scalability of the approach.

Note that such approaches which make use of liquid−air interfaces are exceptionally smooth with roughness measured to be of the order of the nanometer[78]. These fluidic methodologies are thus suitable for applications where precision is paramount, i.e., in optics, where they can produce a broad range of components that do not require polishing before use.[78]

PIXELATED SHEETS

Capillary forces can also be harnessed to generate movement in liquids, as commonly observed when plunging a straw into a glass of water.[48] In this mundane problem, capillary forces and

https://doi.org/10.1021/jacsau.2c00427
JACS Au 2022, 2, 2417−2425

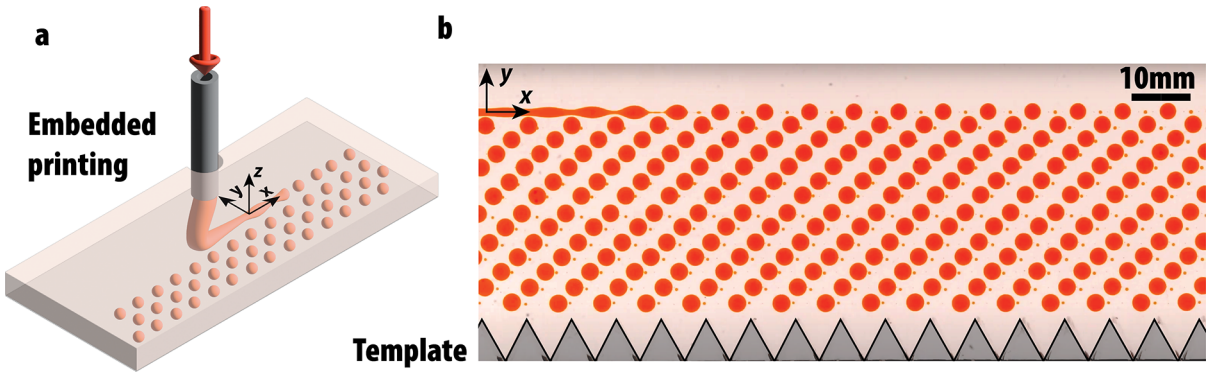

Figure 6. Self-assembled drop crystals. (a) The sequential breakup of viscous threads sequentially printed into another immiscible viscous bath leads to the assembly of a regular lattice of drops. (b) Experimental picture of such a lattice, here driven by the presence of a template (drops are ∼3 mm in diameter).

wetting conditions lead to the formation of a meniscus whose curvature yields a pressure gradient in the liquid, causing the so-called capillary rise. Similar forces are harnessed in the natural world, e.g., in several creatures' drinking strategies.[49] These capillary suction mechanisms can also be leveraged in the laboratory to assemble pixelated materials.[50] In Figure 5a, we show how suction flows can be obtained in a Hele-Shaw cell that consists of two plates separated by a small gap. Here the top plate presents a series of holes, from which the flows proceed until they meet at the dividing lines. As a result, we obtain a Voronoi tessellation (Figure 5b). After curing is complete, these patterns solidify into composite elastic sheets. This method is conceptually analogous to the watershed transform traditionally employed in image analysis and, as such, can be generalized to a variety of source shapes[50] and materials.[50−52] Note that such regular shapes are not exclusive to these carefully engineered settings but can also naturally emerge from mechanical instabilities, as detailed next.

A PARADIGM SHIFT

Mechanical instabilities in engineered structures, e.g., buckling and wrinkling, have historically been perceived as failure mechanisms, such that an enduring motivation for their study has been the desire to avoid them. Recently, however, we have witnessed a paradigm shift wherein mechanical instabilities[53,54] are instead sought after owing to their ability to produce regular patterns that would otherwise be difficult to achieve.[55] Interestingly, this approach has been applied for a long time in the field of inkjet printing. First introduced commercially by Siemens in 1951,[56] continuous inkjet printers have long relied on the Rayleigh−Plateau instability (RPI) to break a liquid jet emerging from a high-pressure reservoir into a multitude of uniformly sized droplets.[4] As such, the RPI has been extensively studied in the context of liquid jets in the air, but also in systems where the outer phase is viscous,[57,58] while the radius of drops formed by the RPI may range anywhere from a few millimeters tenth of nanometers.[59] Techniques such as coflows, the coaxial flow of two immiscible fluids, are now routinely used to disperse a phase (the inner fluid) into a continuous phase (the outer fluid) using stresses of hydrodynamic origin[60−62], and the large range of breaking patterns[63,64] they exhibit are well understood.[65] However, previous research has primarily focused on single threads, leaving recursive mechanisms and collective instabilities in multithread systems poorly understood.[66]

Additionally, classical hydrodynamics focuses on pure liquids. Fluid dynamical systems involving liquids out of equilibrium have been comparatively less explored. Here we discuss how the solid−liquid phase transition inherent to a wide range of materials coupled to carefully designed interfacial flows offers new possibilities in the assembly of complex structures by enabling the harnessing of fluidic instabilities in order to produce solid structures with robust and regular properties.

RAYLEIGH−PLATEAU INSTABILITY

As discussed earlier, drop and droplets have long been harnessed in engineering, being the backbone of tremendously successful technologies such as inkjet printing.[3] Droplets are also key players in the laboratory where they have helped the development lab-on-chip technology.[64] In all these cases, droplets are primarily used as tiny fluids reservoirs, which thereby transport minute and well controlled volumes of liquids. However, droplets can also be leveraged for their shape, e.g., when they serve as templates in bottom up fabrication paradigms.[6,67] In these applications, controlling the monodispersity of the drops is also essential as it informs the structures that emerge when droplets are packed together. This assembly is typically achieved by progressively sucking the continuous phase in which the droplets sit, yielding a hexagonal lattice. While the fabrication of such well-calibrated drops is amenable to existing fluid manipulation paradigms, the self-assembly of droplet lattices is typically limited to densely packed structures with hexagonal symmetries. It has recently been demonstrated that this limitation in structural versatility can be overcome when combining freeform fabrication techniques, such as embedded 3D printing[68] and microfluidics approaches.[69,70] Specifically, when a viscous thread is extruded into another immiscible liquid following a raster toolpath. Leveraging this approach, Cai et al.[69] have indeed shown that the sequential breakup of closely spaced liquid threads locks into crystal-like lattices of droplets (Figure 6). The geometry and composition of the drop lattices can be tuned via the modulation of the printing parameters. Polymerizing the outer phase then yields elastic slabs patterned with liquid inclusions. In turn, these inclusions can be leveraged to induce mechanical deformations[71] and locally modulate the mechanical properties of the media[72] or its acoustic properties.[73]

RAYLEIGH−TAYLOR INSTABILITY

Mechanisms for droplet formation are not limited to the RPI. For instance, a thin coating applied on the underside of a flat substrate will destabilize into a network of droplets following the action of gravity, an instability known as the Rayleigh−Taylor

https://doi.org/10.1021/jacsau.2c00427
JACS Au 2022, 2, 2417−2425

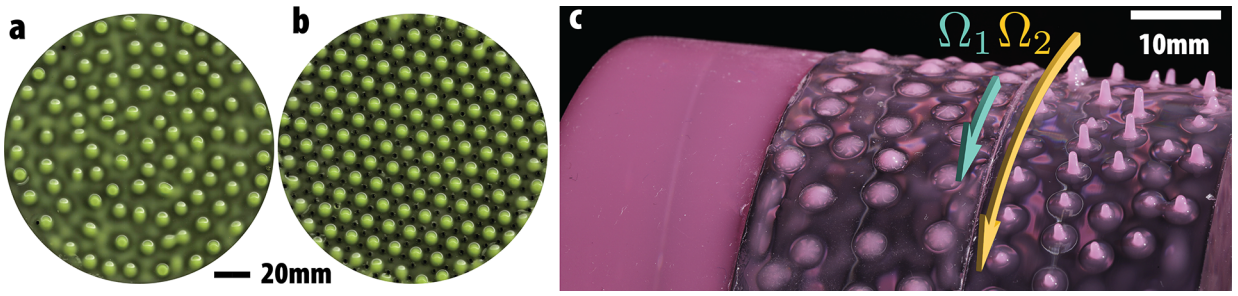

Figure 7. Harnessing the Rayleigh−Taylor instability: (a) Drop pattern forming in a thin polymer film coated on the underside of a flat substrate. (b) This pattern can be made regular using seeds. (c) Photographs of a film applied to a cylinder (left), and the RTI-mediated drops that form when the rotation speed is Ω_1 (middle). Increasing the speed to a larger value Ω_2 during curing yields hair-like elongated structures (right).

instability[74] (RTI, Figure 7a). Likewise, coatings applied to the outside of a rapidly rotating cylinder will form similar kinds of droplets whose spacing follows the most unstable mode of the instability $2\pi\sqrt{2\sigma/\rho a}$, where σ is the liquid interfacial tension, ρ is its density, and a is the magnitude of the centrifugal acceleration acting on the system. As such, changing the magnitude of the acceleration field a diminishes the size of the droplets that the RTI forms. Structures down to a few micrometers have been demonstrated.[75] Of particular interest for fabrication purposes is the possibility of controlling the arrangement of these drops relative to each other. Specifically, it has been shown that the lattice type can be dictated by using carefully crafted defects seeded in the substrate prior to coating (Figure 7b).[75] The shape of the drops can also be altered, this time using a modulation of the acceleration field over the course of an experiment.[76] This modulation is typically applied at the gelation point of the polymer used in the experiment, i.e., when the elastomer is no longer liquid but still much softer than it will eventually be when fully cured. Hair-like elongated structures then grow as the initially formed drops are stretched due to the increased acceleration (Figure 7c). This acceleration is maintained constant for the remainder of the curing process. The elastomer shear modulus then progressively increases by over 3 orders of magnitude. As the acceleration stops, curing is complete and this moldless approach yields a forest of hair at the surface of the substrate.[76] Note that these structures arise from the coupling of concomitant effects: the mechanical deformation that follows the RTI and the curing of the elastomer that pertains to chemical reactions occurring at the molecular level of the polymer.

DISCUSSION AND CONCLUSIONS

In this Perspective, we have primarily discussed interfacial flows in the context of curable elastomers. We have highlighted the *universality* of these processes capable of memory loss (insensitive to initial conditions) and yielding the robust assembly of periodic structures obtained following relatively simple design guidelines (insensitive to materials properties). However, we note that the directed control of these flows is still in its infancy. A combination of experimental, theoretical, and numerical efforts is still needed to provide a unified description of this class of problems and solutions to the so-called inverse design problem: finding the set of initial and boundary conditions[69,77] such that a liquid mixture would flow and solidify into arbitrarily complex target shapes (three-dimensional and multimaterial). Efforts in Chemistry are needed to better understand and ultimately better engineer reversible, stimuli-responsive, and controllable cross-linking mixtures. For instance, advances to rationalize the link between molecular processes occurring in these crowded environments and the effective time varying macroscopic behavior of these solutions would be instrumental to further develop the fabrications methods we have discussed. Achieving such a feat would have tremendous technological value. The idea of arresting flows for reliable design and fabrication of self-organized patterns indeed goes far beyond the specific phenomena and liquids discussed in this Perspective. This burgeoning movement is targeting a broad range of phenomena to develop moldless methodologies for assembling optical components,[78] porous materials,[79] textiles,[80] pharmaceutical particles,[81] and fractal and chaotic structures.[82−85] This type of approach is potentially applicable to a broad range of liquids from commodity/engineering materials (e.g., thermoplastics/thermosets), to innovative materials such as responsive hydrogels[86] and liquid crystal elastomers,[87] to UV curable solutions,[88] to bioactive materials,[89] to cellulose-based materials,[90] and to ceramics and metals.[91,92] Of particular interest to technological applications is that the resolution of fluid-mediated assemblies relies on the physics of fluids, e.g., in contrast with printing, where the resolution of the print directly scales with the size of the deposition nozzle and the accuracy of the hardware directing its motion. Instead, the solids we discussed are smooth down to the limit of continuum mechanics.[78] Additionally, pattern formation in this class of systems is intrinsically scalable. For instance, think of the vast areas covered by mud cracks, sand ripples, and other geomorphic features seen on earth and other planets,[93−97] which are all the result of instabilities. Finally, these processes are frugal. The structures we discussed primarily stem from passively harnessing gravity and interfacial effects at room temperature, thereby yielding minimal energy expenditures. As a consequence, these processes could nicely complement existing fabrication paradigms. An immediate application would be the manipulation of viscous solutions (1 Pa·s and above) and extreme materials (e.g., molten glass, as discussed in this Perspective). Comparatively, inkjet printing is limited to operating in a narrow range of viscosities (∼1 mPa·s) and requires surfactants to fine-tune the surface tension of the ink. Likewise, large throughputs in microfluidic systems are only possible with polymers in a low-viscosity state (below 100 mPa·s), while the solutions typically processed into particles for materials design are rather viscous.[98]

In closing, we note that the distribution of geometrically engineered materials in our daily lives remains very limited due to the difficulty of assembling such structures. The fluidic approaches discussed in this Perspective could help address the challenge of developing scalable fabrication processes that are

https://doi.org/10.1021/jacsau.2c00427
JACS Au 2022, 2, 2417−2425

sufficiently versatile to bridge the millimetric and micro- or even nanoscale, compatible with various liquids, and that can produce a multiplicity of architectures for specific engineering applications. Interfacial flows and instabilities can comfortably handle length scales ranging from ∼1 μm to ∼1 m while coupling these pattern-forming systems to complex fluids, e.g., embarking binary mixtures,[99] colloid suspensions, or nano-fillers,[100] would open the door to truly multiscale designs. The flow would have the dual purpose of shaping the overall structure and interface of the material while providing the means and the conditions, e.g., via shear, for order to arise at the smallest scales.

AUTHOR INFORMATION

Corresponding Author

Pierre-Thomas Brun − *Department of Chemical and Biological Engineering, Princeton University, Princeton, New Jersey 08540, United States;* orcid.org/0000-0002-4175-0604; Email: pbrun@princeton.edu

Complete contact information is available at: https://pubs.acs.org/10.1021/jacsau.2c00427

Notes

The author declares the following competing financial interest(s): The bubble casting methodology described in this manuscript is the subject of a US provisional patent application filed by Princeton University on behalf of the author (no. 63/354,538).

ACKNOWLEDGMENTS

The author acknowledges the final support of the National Science Foundation, NSF CAREER award (CBET 2042930) and NSF FMRG award (CMMI 2037097), for financial support during the writing of this manuscript. This publication was supported by the Princeton University Library Open Access Fund. The author thanks Prof. Doug Holmes for his constructive comments on polymer chemistry.

REFERENCES

(1) de Gennes, P.-G.; Brochard-Wyart, F.; Quéré, D.*Capillarity and Wetting Phenomena, Drops, Bubbles, Pearls, Waves*; Springer, 2004. DOI: 10.1007/978-0-387-21656-0.

(2) Pilkington, L. A. B. Review Lecture: The Float Glass Process. *Proc. Royal Soc. London Math Phys. Sci.* **1969**, *314* (1516), 1−25.

(3) Lohse, D. Fundamental Fluid Dynamics Challenges in Inkjet Printing. *Annu. Rev. Fluid Mech.* **2021**, *54*, 349.

(4) Eggers, J.; Villermaux, E. Physics of Liquid Jets. *Rep. Prog. Phys.* **2008**, *71* (3), 036601.

(5) Stone, H. A.; Stroock, A. D.; Ajdari, A. Engineering Flows in Small Devices. *Annu. Rev. Fluid Mech* **2004**, *36* (1), 381−411.

(6) Fernandez-Nieves, A., Puertas, A. M., Eds. *Fluids, Colloids and Soft Materials: An Introduction to Soft Matter Physics*; Wiley, 2016.

(7) Utada, A. S.; Lorenceau, E.; Link, D. R.; Kaplan, P. D.; Stone, H. A.; Weitz, D. A. Monodisperse Double Emulsions Generated from a Microcapillary Device. *Science* **2005**, *308* (5721), 537−541.

(8) Utada, A. S.; Fernandez-Nieves, A.; Stone, H. A.; Weitz, D. A. Dripping to Jetting Transitions in Coflowing Liquid Streams. *Phys. Rev. Lett.* **2007**, *99* (9), 094502.

(9) Py, C.; Reverdy, P.; Doppler, L.; Bico, J.; Roman, B.; Baroud, C. N. Capillary Origami: Spontaneous Wrapping of a Droplet with an Elastic Sheet. *Phys. Rev. Lett.* **2007**, *98* (15), 156103.

(10) Evans, A. A.; Spagnolie, S. E.; Bartolo, D.; Lauga, E. Elastocapillary Self-Folding: Buckling, Wrinkling, and Collapse of Floating Filaments. *Soft Matter* **2013**, *9* (5), 1711−1720.

(11) Roman, B.; Bico, J. Elasto-Capillarity: Deforming an Elastic Structure with a Liquid Droplet. *J. Phys.: Condens. Matter* **2010**, *22* (49), 493101.

(12) Bico, J.; Reyssat, É.; Roman, B. Elastocapillarity: When Surface Tension Deforms Elastic Solids. *Annu. Rev. Fluid Mech* **2018**, *50*, 629.

(13) Li, S.; Deng, B.; Grinthal, A.; Schneider-Yamamura, A.; Kang, J.; Martens, R. S.; Zhang, C. T.; Li, J.; Yu, S.; Bertoldi, K.; Aizenberg, J. Liquid-Induced Topological Transformations of Cellular Microstructures. *Nature* **2021**, *592* (7854), 386−391.

(14) Gallaire, F.; Brun, P.-T. Fluid Dynamic Instabilities: Theory and Application to Pattern Forming in Complex Media. *Philos. Trans. R. Soc. Math Phys. Eng. Sci.* **2017**, *375* (2093), 20160155.

(15) Villermaux, E. The Formation of Filamentary Structures from Molten Silicates: Pele's Hair, Angel Hair, and Blown Clinker. *Comptes Rendus Mécanique* **2012**, *340* (8), 555−564.

(16) Truby, R. L.; Lewis, J. A. Printing Soft Matter in Three Dimensions. *Nature* **2016**, *540* (7633), 371−378.

(17) Skylar-Scott, M. A.; Mueller, J.; Visser, C. W.; Lewis, J. A. Voxelated Soft Matter via Multimaterial Multinozzle 3D Printing. *Nature* **2019**, *575* (7782), 330−335.

(18) Xia, Y.; Whitesides, G. M. Soft Lithography. *Annu. Rev. Mater. Sci.* **1998**, *28* (1), 153−184.

(19) Kim, S. O.; Solak, H. H.; Stoykovich, M. P.; Ferrier, N. J.; Pablo, J. J.; de Nealey, P. F. Epitaxial Self-Assembly of Block Copolymers on Lithographically Defined Nanopatterned Substrates. *Nature* **2003**, *424* (6947), 411−414.

(20) Whitesides, G. M.; Grzybowski, B. Self-Assembly at All Scales. *Science* **2002**, *295* (5564), 2418−2421.

(21) Cera, L.; Gonzalez, G. M.; Liu, Q.; Choi, S.; Chantre, C. O.; Lee, J.; Gabardi, R.; Choi, M. C.; Shin, K.; Parker, K. K. A Bioinspired and Hierarchically Structured Shape-Memory Material. *Nat. Mater.* **2021**, 242.

(22) Naleway, S. E.; Porter, M. M.; McKittrick, J.; Meyers, M. A. Structural Design Elements in Biological Materials: Application to Bioinspiration. *Adv. Mater.* **2015**, *27* (37), 5455−5476.

(23) Bhushan, B. Biomimetics: Lessons from Nature−an Overview. *Philosophical Transactions Royal Soc. Math Phys. Eng. Sci.* **2009**, *367*, 1445−1486.

(24) Cross, M. C.; Hohenberg, P. C. Pattern Formation Outside of Equilibrium. *Rev. Mod. Phys.* **1993**, *65* (3), 851−1112.

(25) Vella, D. Floating Versus Sinking. *Annu. Rev. Fluid Mech.* **2015**, *47*, 115.

(26) Andreotti, B.; Forterre, Y.; Pouliquen, O.Geomorphology. In *Granular Media*; Cambridge University Press, 2013; pp 363−431. .

(27) Brau, F.; Vandeparre, H.; Sabbah, A.; Poulard, C.; Boudaoud, A.; Damman, P. Multiple-Length-Scale Elastic Instability Mimics Parametric Resonance of Nonlinear Oscillators. *Nat. Phys.* **2011**, *7* (1), 56−60.

(28) Marthelot, J.; Roman, B.; Bico, J.; Teisseire, J.; Dalmas, D.; Melo, F. Self-Replicating Cracks: A Collaborative Fracture Mode in Thin Films. *Phys. Rev. Lett.* **2014**, *113* (8), 085502.

(29) Brun, P.-T. A Sticky Situation. *J. Fluid Mech.* **2017**, *820*, 1−4.

(30) Brun, P.-T.; Audoly, B.; Ribe, N. M.; Eaves, T. S.; Lister, J. R. Liquid Ropes: A Geometrical Model for Thin Viscous Jet Instabilities. *Phys. Rev. Lett.* **2015**, *114* (17), 174501.

(31) Jawed, M. K.; Da, F.; Joo, J.; Grinspun, E.; Reis, P. M. Coiling of Elastic Rods on Rigid Substrates. *Proc. National Acad. Sci.* **2014**, *111* (41), 14663−14668.

(32) Jawed, M. K.; Brun, P.-T.; Reis, P. M. A Geometric Model for the Coiling of an Elastic Rod Deployed Onto a Moving Substrate. *J. Appl. Mech* **2015**, *82* (12), 121007.

(33) Lister, J. R.; Chiu-Webster, S. The Fall of a Viscous Thread onto a Moving Surface: A 'Fluid-Mechanical Sewing Machine. *J. Fluid Mech.* **2006**, *569*, 89−111.

(34) Morris, S. W.; Dawes, J. H. P.; Ribe, N. M.; Lister, J. R. Meandering Instability of a Viscous Thread. *Phys. Rev. E* **2008**, *77* (6), 066218.

(35) Brun, P.-T.; Ribe, N. M.; Audoly, B. A Numerical Investigation of the Fluid Mechanical Sewing Machine. *Phys. Fluids* **2012**, *24* (4), 043102.
(36) Passieux, R.; Guthrie, L.; Rad, S. H.; Lévesque, M.; Therriault, D.; Gosselin, F. P. Instability-Assisted Direct Writing of Microstructured Fibers Featuring Sacrificial Bonds. *Adv. Mater.* **2015**, *27* (24), 3676−3680.
(37) Jawed, M. K.; Hadjiconstantinou, N. G.; Parks, D. M.; Reis, P. M. Patterns of Carbon Nanotubes by Flow-Directed Deposition on Substrates with Architectured Topographies. *Nano Lett.* **2018**, *18* (3), 1660−1667.
(38) Yuk, H.; Zhao, X. A New 3D Printing Strategy by Harnessing Deformation, Instability, and Fracture of Viscoelastic Inks. *Adv. Mater.* **2018**, *30* (6), 1704028.
(39) Lipton, J. I.; Lipson, H. 3D Printing Variable Stiffness Foams Using Viscous Thread Instability. *Sci. Rep-uk* **2016**, *6* (1), 29996.
(40) Brun, P.-T.; Inamura, C.; Lizardo, D.; Franchin, G.; Stern, M.; Houk, P.; Oxman, N. The Molten Glass Sewing Machine. *Philosophical Transactions Royal Soc. Math Phys. Eng. Sci.* **2017**, *375*, 20160156.
(41) Zheng, P.; McCarthy, T. J. Rediscovering Silicones: Molecularly Smooth, Low Surface Energy, Unfilled, UV/Vis-Transparent, Extremely Cross-Linked, Thermally Stable, Hard, Elastic PDMS. *Langmuir* **2010**, *26* (24), 18585−18590.
(42) Schleifer, J.; Marthelot, J.; Jones, T. J.; Brun, P.-T. The Fingerprint of a Flow: Wrinkle Patterns in Nonuniform Coatings on Pre-Stretched Soft Foundations. *Soft Matter* **2019**, *15* (6), 1405−1412.
(43) Jones, T. J.; Jambon-Puillet, E.; Marthelot, J.; Brun, P.-T. Bubble Casting Soft Robotics. *Nature* **2021**, *599* (7884), 229−233.
(44) Lee, A.; Brun, P.-T.; Marthelot, J.; Balestra, G.; Gallaire, F.; Reis, P. M. Fabrication of Slender Elastic Shells by the Coating of Curved Surfaces. *Nat. Commun.* **2016**, *7* (1), 11155.
(45) Sahu, N.; Parija, B.; Panigrahi, S. Fundamental Understanding and Modeling of Spin Coating Process: A Review. *Indian J. Phys.* **2009**, *83* (4), 493−502.
(46) Marthelot, J.; Brun, P.-T.; Jiménez, F. L.; Reis, P. M. Reversible Patterning of Spherical Shells through Constrained Buckling. *Phys. Rev. Mater.* **2017**, *1* (2), 025601.
(47) Lee, A.; Jiménez, F. L.; Marthelot, J.; Hutchinson, J. W.; Reis, P. M. The Geometric Role of Precisely Engineered Imperfections on the Critical Buckling Load of Spherical Elastic Shells. *J. Appl. Mech* **2016**, *83* (11), 111005.
(48) de Gennes, P.-G.; Brochard-Wyart, F.; Quéré, D.*Capillarity and Wetting Phenomena, Drops, Bubbles, Pearls, Waves*; Springer, 2004; pp 33−67.
(49) Kim, W.; Bush, J. W. M. Natural Drinking Strategies. *J. Fluid Mech.* **2012**, *705*, 7−25.
(50) Badaoui, M.; Kresge, G.; Ushay, C.; Marthelot, J.; Brun, P.-T. Formation of Pixelated Elastic Films via Capillary Suction of Curable Elastomers in Templated Hele-Shaw Cells. *Adv. Mater.* **2022**, *34*, 2109682.
(51) Goyette, P.-A.; Boulais, É.; Tremblay, M.; Gervais, T. Pixel-Based Open-Space Microfluidics for Versatile Surface Processing. *Proc. National Acad. Sci.* **2021**, *118* (2), e2019248118.
(52) Heinrich, M. A.; Alert, R.; Wolf, A. E.; Košmrlj, A.; Cohen, D. J. Self-Assembly of Tessellated Tissue Sheets by Expansion and Collision. *Nat. Commun.* **2022**, *13* (1), 4026.
(53) Reis, P. M. A Perspective on the Revival of Structural (In)Stability With Novel Opportunities for Function: From Buckliphobia to Buckliphilia. *J. Appl. Mech* **2015**, *82* (11), 111001.
(54) Bertoldi, K.; Vitelli, V.; Christensen, J.; van Hecke, M. Flexible Mechanical Metamaterials. *Nat. Rev. Mater.* **2017**, *2*, 170666.
(55) Yang, S.; Khare, K.; Lin, P. Harnessing Surface Wrinkle Patterns in Soft Matter. *Adv. Funct Mater.* **2010**, *20* (16), 2550−2564.
(56) Elmqvist, R. US Patent US2566443.
(57) Stone, H. A.; Brenner, M. P. Note on the Capillary Thread Instability for Fluids of Equal Viscosities. *J. Fluid Mech.* **1996**, *318* (1), 373−374.
(58) Tomotika, S. On the Instability of a Cylindrical Thread of a Viscous Liquid Surrounded by Another Viscous Fluid. *Proc. Royal Soc. Lond Ser. - Math Phys. Sci.* **1935**, *150*, 322−337.
(59) Kaufman, J. J.; Tao, G.; Shabahang, S.; Banaei, E.-H.; Deng, D. S.; Liang, X.; Johnson, S. G.; Fink, Y.; Abouraddy, A. F. Structured Spheres Generated by an In-Fibre Fluid Instability. *Nature* **2012**, *487* (7408), 463.
(60) Castro-Hernández, E.; Campo-Cortés, F.; Gordillo, J. M. Slender-Body Theory for the Generation of Micrometre-Sized Emulsions through Tip Streaming. *J. Fluid Mech.* **2012**, *698*, 423−445.
(61) Gordillo, J. M.; Sevilla, A.; Campo-Cortés, F. Global Stability of Stretched Jets: Conditions for the Generation of Monodisperse Micro-Emulsions Using Coflows. *J. Fluid Mech.* **2014**, *738*, 335−357.
(62) Evangelio, A.; Campo-Cortés, F.; Gordillo, J. M. Simple and Double Microemulsions via the Capillary Breakup of Highly Stretched Liquid Jets. *J. Fluid Mech.* **2016**, *804*, 550−577.
(63) Cubaud, T.; Mason, T. G. Capillary Threads and Viscous Droplets in Square Microchannels. *Phys. Fluids* **2008**, *20* (5), 053302.
(64) Baroud, C. N.; Gallaire, F.; Dangla, R. Dynamics of Microfluidic Droplets. *Lab Chip* **2010**, *10* (16), 2032−2045.
(65) Nunes, J. K.; Tsai, S. S. H.; Wan, J.; Stone, H. A. Dripping and Jetting in Microfluidic Multiphase Flows Applied to Particle and Fibre Synthesis. *J. Phys. D Appl. Phys.* **2013**, *46* (11), 114002.
(66) Mansard, V.; Mecca, J. M.; Dermody, D. L.; Malotky, D.; Tucker, C. J.; Squires, T. M. Collective Rayleigh-Plateau Instability: A Mimic of Droplet Breakup in High Internal Phase Emulsion. *Langmuir* **2016**, *32* (11), 2549−2555.
(67) Du, H.; Cont, A.; Steinacher, M.; Amstad, E. Fabrication of Hexagonal-Prismatic Granular Hydrogel Sheets. *Langmuir* **2018**, *34* (11), 3459−3466.
(68) Muth, J. T.; Vogt, D. M.; Truby, R. L.; Mengüç, Y.; Kolesky, D. B.; Wood, R. J.; Lewis, J. A. Embedded 3D Printing of Strain Sensors within Highly Stretchable Elastomers. *Adv. Mater.* **2014**, *26* (36), 6307−6312.
(69) Cai, L.; Marthelot, J.; Brun, P.-T. Instability Mediated Self-Templating of Drop Crystals. *Sci. Adv.* **2022**, *8* (27), eabq0828.
(70) Cai, L.; Marthelot, J.; Brun, P.-T. An Unbounded Approach to Microfluidics Using the Rayleigh−Plateau Instability of Viscous Threads Directly Drawn in a Bath. *Proc. National Acad. Sci.* **2019**, *116* (46), 22966−22971.
(71) Cai, L.; Marthelot, J.; Falcón, C.; Reis, P. M.; Brun, P.-T. Printing on Liquid Elastomers. *Soft Matter* **2020**, *16* (12), 3137−3142.
(72) Style, R. W.; Boltyanskiy, R.; Allen, B.; Jensen, K. E.; Foote, H. P.; Wettlaufer, J. S.; Dufresne, E. R. Stiffening Solids with Liquid Inclusions. *Nat. Phys.* **2015**, *11* (1), 82−87.
(73) Brunet, T.; Leng, J.; Mondain-Monval, O. Soft Acoustic Metamaterials. *Science* **2013**, *342* (6156), 323−324.
(74) Fermigier, M.; Limat, L.; Wesfreid, J. E.; Boudinet, P.; Quilliet, C. Two-Dimensional Patterns in Rayleigh-Taylor Instability of a Thin Layer. *J. Fluid Mech.* **1992**, *236* (1), 349−383.
(75) Marthelot, J.; Strong, E. F.; Reis, P. M.; Brun, P.-T. Designing Soft Materials with Interfacial Instabilities in Liquid Films. *Nat. Commun.* **2018**, *9* (1), 4477.
(76) Jambon-Puillet, E.; Piéchaud, M. R.; Brun, P.-T. Elastic Amplification of the Rayleigh−Taylor Instability in Solidifying Melts. *Proc. National Acad. Sci.* **2021**, *118* (10), e2020701118.
(77) Ledda, P. G.; Lerisson, G.; Balestra, G.; Gallaire, F. Instability of a Thin Viscous Film Flowing under an Inclined Substrate: The Emergence and Stability of Rivulets. *J. Fluid Mech.* **2020**, *904*, A23.
(78) Frumkin, V.; Bercovici, M. Fluidic Shaping of Optical Components. *Flow* **2021**, *1*, E2.
(79) Dent, F. J.; Harbottle, D.; Warren, N. J.; Khodaparast, S. Temporally Arrested Breath Figure. *Acs Appl. Mater. Inter* **2022**, *14* (23), 27435−27443.
(80) Iqbal, S.; MacLean, K.; Chevalier, F.; Mueller, S.; Forman, J.; Dogan, M. D.; Forsythe, H.; Ishii, H. DefeXtiles. *Proc. 33rd Annu. ACM Symp. User Interface Software Technol.* **2020**, 1222−1233.

https://doi.org/10.1021/jacsau.2c00427
JACS Au 2022, 2, 2417−2425

(81) Nelson, A. Z.; Kundukad, B.; Wong, W. K.; Khan, S. A.; Doyle, P. S. Embedded Droplet Printing in Yield-Stress Fluids. *Proc. National Acad. Sci.* **2020**, *117* (11), 5671−5679.
(82) Roh, S.; Williams, A. H.; Bang, R. S.; Stoyanov, S. D.; Velev, O. D. Soft Dendritic Microparticles with Unusual Adhesion and Structuring Properties. *Nat. Mater.* **2019**, *18* (12), 1315−1320.
(83) Chakrabarti, A.; Al-Mosleh, S.; Mahadevan, L. Instabilities and Patterns in a Submerged Jelling Jet. *Soft Matter* **2021**, *17* (42), 9745−9754.
(84) Islam, T. ul; Gandhi, P. S. Fabrication of Multscale Fractal-Like Structures by Controlling Fluid Interface Instability. *Sci. Rep-uk* **2016**, *6* (1), 37187.
(85) Islam, T. ul; Gandhi, P. S. Viscous Fingering in Multiport Hele Shaw Cell for Controlled Shaping of Fluids. *Sci. Rep-uk* **2017**, *7* (1), 16602.
(86) Gladman, A. S.; Matsumoto, E. A.; Nuzzo, R. G.; Mahadevan, L.; Lewis, J. A. Biomimetic 4D Printing. *Nat. Mater.* **2016**, *15* (4), 413−418.
(87) Wang, Y.; Liu, J.; Yang, S. Multi-Functional Liquid Crystal Elastomer Composites. *Appl. Phys. Rev.* **2022**, *9* (1), 011301.
(88) Perazzo, A.; Nunes, J. K.; Guido, S.; Stone, H. A. Flow-Induced Gelation of Microfiber Suspensions. *Proc. National Acad. Sci.* **2017**, *114* (41), E8557−E8564.
(89) Nerger, B. A.; Brun, P.-T.; Nelson, C. M. Marangoni Flows Drive the Alignment of Fibrillar Cell-Laden Hydrogels. *Sci. Adv.* **2020**, *6* (24), eaaz7748.
(90) Giachini, P. A. G. S.; Gupta, S. S.; Wang, W.; Wood, D.; Yunusa, M.; Baharlou, E.; Sitti, M.; Menges, A. Additive Manufacturing of Cellulose-Based Materials with Continuous, Multidirectional Stiffness Gradients. *Sci. Adv.* **2020**, *6* (8), eaay0929.
(91) Mowlavi, S.; Shukla, I.; Brun, P.-T.; Gallaire, F. Particle Size Selection in Capillary Instability of Locally Heated Coaxial Fiber. *Phys. Rev. Fluids* **2019**, *4* (6), 064003.
(92) Song, M.; Kartawira, K.; Hillaire, K. D.; Li, C.; Eaker, C. B.; Kiani, A.; Daniels, K. E.; Dickey, M. D. Overcoming Rayleigh−Plateau Instabilities: Stabilizing and Destabilizing Liquid-Metal Streams via Electrochemical Oxidation. *Proc. National Acad. Sci.* **2020**, *117* (32), 19026−19032.
(93) Claudin, P.; Durán, O.; Andreotti, B. Dissolution Instability and Roughening Transition. *J. Fluid Mech.* **2017**, *832*, R2.
(94) Andreotti, B.; Forterre, Y.; Pouliquen, O.Foreword. In *Granular Media*; Cambridge University Press, 2009; pp vii−viii.
(95) Moores, J. E.; Smith, C. L.; Toigo, A. D.; Guzewich, S. D. Penitentes as the Origin of the Bladed Terrain of Tartarus Dorsa on Pluto. *Nature* **2017**, *541* (7636), 188−190.
(96) Huang, J. M.; Tong, J.; Shelley, M.; Ristroph, L. Ultra-Sharp Pinnacles Sculpted by Natural Convective Dissolution. *Proc. National Acad. Sci.* **2020**, *117* (38), 23339−23344.
(97) Ledda, P. G.; Balestra, G.; Lerisson, G.; Scheid, B.; Wyart, M.; Gallaire, F. Hydrodynamic-Driven Morphogenesis of Karst Draperies: Spatio-Temporal Analysis of the Two-Dimensional Impulse Response. *J. Fluid Mech.* **2021**, *910*, A53.
(98) Håti, A. G.; Szymborski, T. R.; Steinacher, M.; Amstad, E. Production of Monodisperse Drops from Viscous Fluids. *Lab Chip* **2018**, *18* (4), 648−654.
(99) Lohse, D.; Zhang, X. Physicochemical Hydrodynamics of Droplets out of Equilibrium. *Nat. Rev. Phys.* **2020**, *2* (8), 426−443.
(100) Zhao, C.; Zhang, P.; Zhou, J.; Qi, S.; Yamauchi, Y.; Shi, R.; Fang, R.; Ishida, Y.; Wang, S.; Tomsia, A. P.; Liu, M.; Jiang, L. Layered Nanocomposites by Shear-Flow-Induced Alignment of Nanosheets. *Nature* **2020**, *580* (7802), 210−215.

https://doi.org/10.1021/jacsau.2c00427
JACS Au 2022, 2, 2417−2425